

# New Predistortion Linearizer Using Low-Frequency Even-Order Intermodulation Components

Youngoo Yang, *Student Member, IEEE*, Young Yun Woo, and Bumman Kim, *Senior Member, IEEE*

**Abstract**—We present two types of new predistortion linearizers using low-frequency even-order components. One adopts an in-phase and quadrature balanced modulator as a generator of the third-order intermodulation (IM3) and fifth-order intermodulation (IM5) components and the other adopts a double-balanced diode mixer. Both types are very compact and could independently control the amplitudes and phases of the intermodulation (IM) components. We have analyzed the delay mismatch effect of these predistortion circuits. The result shows that the IM5 components are twice as sensitive than the third ones. Two types of predistorters are implemented and tested at the International Mobile Telecommunications-2000 band. Two tone test results show that the IM3 cancellation is about 23–25 dB and the IM5 is cancelled by about 12–20 dB for both cases. The adjacent channel power ratio is improved by over 11 dB at the broad-band CDMA signal with a chip rate of 4.096 Mc/s, and this improvement is maintained through a broad range of output power level.

**Index Terms**—ACLR, base station, CDMA, feedforward, intermodulation, linearizer, power amplifier, predistortion, MCPA, SCPA.

## I. INTRODUCTION

FOR THE base station of wireless communication systems with varying envelop modulation, such as QPSK or 16 quadrature amplitude modulation (QAM), a highly linear power amplifier is essential. For the multicarrier power amplifiers (MCPAs) of the base station, a feed-forward technique is generally adopted due to its extremely linear and broad-band characteristics. However, the feed-forward technique demands both large and expensive circuits because of its complexity. It has two cancellation paths, delay lines for each path phase adjustment, an auxiliary error amplifier, and a complex control circuit [1]–[8]. Hence, more compact and lower cost linearization techniques, i.e., various predistortion methods [9]–[14], are extensively used for the single-carrier power amplifiers (SCPAs) of the base station and relay systems.

Most of the analog predistortion linearizers have focused on the reduction of the third-order intermodulation (IM3) components. However, the higher order component cancellation becomes more important since the high power amplifiers are generally operated at highly nonlinear class-AB mode. From this point-of-view, new predistortion techniques, which have the capability of independent generation and control of the IM3

and IM5 (fifth-order intermodulation) using low-frequency even-order terms, are proposed. The low-frequency even-order IM (intermodulation) components could generate the odd-order in-band IM terms when they are modulated by the fundamental signal. The even-order harmonics are very low-frequency components and the predistorters based on the concept have very compact circuits and lower gain losses than other analog methods.

A low-frequency second-order IM component ( $\omega_2 - \omega_1$ ) is generated by a nonlinear power amplifier and then the fourth-order component ( $2\omega_2 - 2\omega_1$ ) is generated by multiplying it, using an analog multiplier. We have implemented two circuits for the third and fifth harmonic generations and their controls. In the first circuits, we have used an in-phase and quadrature (I/Q) balanced modulator to properly generate the IM3 and IM5 components. In the second circuits, we have used the nonlinearity of a double-balanced diode mixer as the IM3 and IM5 generator. A description of the proposed circuit topologies and analysis of the delay mismatch effect in the predistorters are presented in Sections II and III. The delay mismatch could lead to a performance degradation in the predistorters due to phase mismatches, but in a different way from a feed-forward method. At the International Mobile Telecommunications-2000 (IMT-2000) frequency band, two-tone tests and broad-band CDMA tests are performed, with the results shown in Section IV. The results prove that the proposed predistortion linearizers have a good capability of independent cancellations of the IM3 and IM5 components of high-power amplifiers.

Generally, the predistortion techniques have three major performance degradation factors, which are not observed in the feed-forward method. These factors could explain the cancellation limit of the predistorter and could offer a design guide. For the two-tone input, these factors are explained as follows.

### A. IMD Characteristic Variations for Different Tone Spacings

It is very difficult to design high-power amplifiers with uniform intermodulation distortion (IMD) characteristics with respect to tone spacings. The characteristic variations can be caused by a large memory effect, a thermal effect, and most importantly, nonuniform band characteristics of the multistage high-power amplifiers [15], [16]. In this case, the optimum IM cancellation point can be slightly different for the different input tone spacings. This limitation could be mitigated by a main amplifier with properly designed bias and harmonic termination circuits to have a uniform IMD characteristics for different tone spacings [15], [16]. However, it is still a tradeoff between simplicity and performance.

Manuscript received May 18, 2000; revised February 15, 2001.

The authors are with the Department of Electronic and Electrical Engineering, Microwave Application Research Center, Pohang University of Science and Technology, Namku Pohang 790-784, Korea (e-mail: alice@postech.ac.kr; bmkim@postech.ac.kr).

Publisher Item Identifier S 0018-9480(02)01156-0.

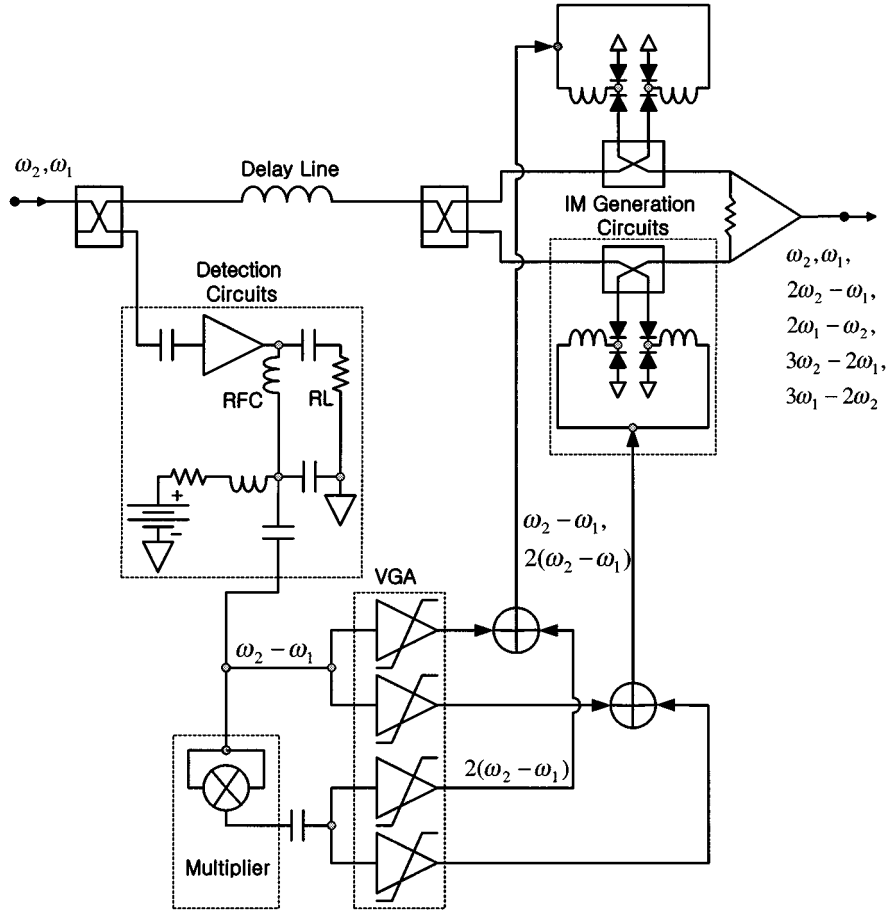


Fig. 1. Block diagram of the new predistortion linearizer using an I/Q balanced modulator as an IM generation circuit.

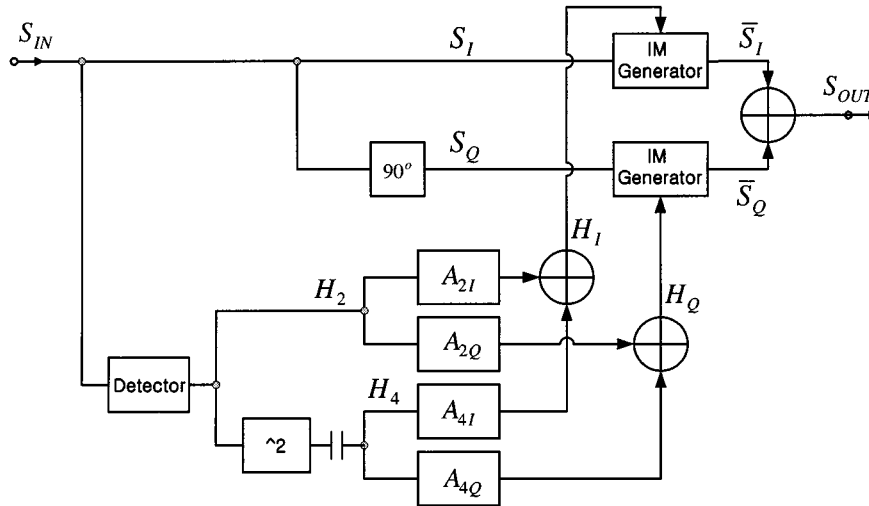


Fig. 2. Operational diagram of the predistorter using an I/Q balanced modulator.

**B. IMD Characteristic Variations With Input Power Levels**

The amplitudes and phases of the IM components of class-AB amplifiers vary rapidly according to the input power level, especially at high-power levels. However, most of the predistorters generate the IM3 and IM5 components using the third- and fifth-order terms of a nonlinear transfer function, respectively. Thus, IM3 and IM5 generated by the predistorter have the gain slope of three and five times larger than that of fundamental

signal, respectively, and have small phase variations along the input power level. Therefore, they cannot cancel the two harmonic components simultaneously for the broad power level.

**C. Effects of Higher Order IM Terms**

General predistorters concentrate on the cancellation of the IM3 component and the more extended ones consider the

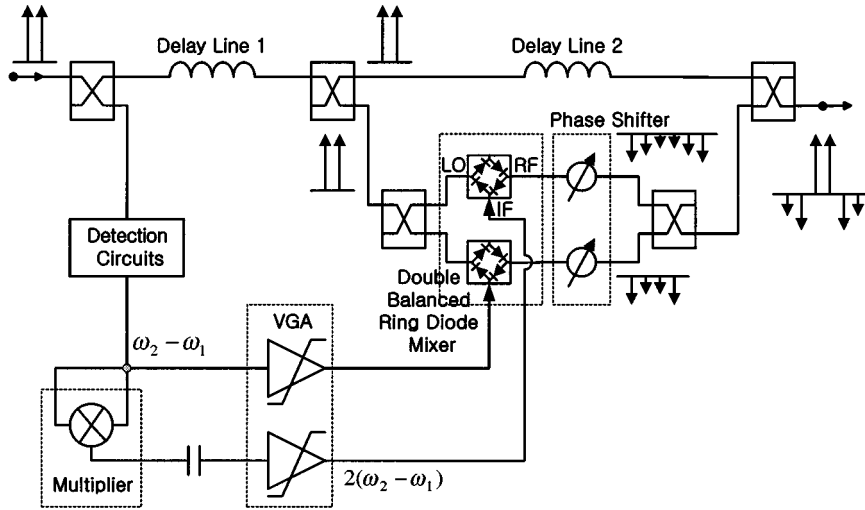


Fig. 3. Block diagram of the new predistortion linearizer using a double-balanced diode mixer as an IM generator.

fifth-order term. The higher order IM components could generate serious distortions, especially for high-power amplifiers.

To design predistortion linearized power amplifiers, a proper consideration of the above-mentioned three degradation factors should be taken into account and appropriate tradeoffs should be made. To develop a good linearized amplifier, the predistorter should have the capability to independently control the amplitude and phase of its IM components with a few tuning parameters and the main amplifier should be designed with consideration of the IM components matched to the predistorter's.

## II. LINEARIZERS

### A. Predistorter Using an I/Q Balanced Modulator

Fig. 1 shows the block diagram of the predistorter using an I/Q balanced modulator as an IM generation circuit. The total circuit has three parts, i.e., the detection circuit, the harmonic control circuit, and the I/Q balanced RF modulator. The detection circuit consists of an RF amplifier, which generates harmonic components. We take the low-frequency second-order IM component ( $\omega_2 - \omega_1$ ) from its drain bias circuit. A series inductor and resistor are connected to choke the  $\omega_2 - \omega_1$  component from the dc voltage source and the dc source is blocked using a large coupling capacitor.

The harmonic control circuit consists of an analog multiplier, which multiplies the  $\omega_2 - \omega_1$  component to make the fourth-order component ( $2\omega_2 - 2\omega_1$ ). The signals are applied to the variable gain amplifier (VGA) through the dc blocking capacitor. It adjusts the phases and amplitudes of the IM3 and IM5 components at the I/Q balanced modulator. The input signal is RF modulated by the low-frequency components in the I/Q mode. The output becomes the input signal with predistortion harmonics.

The operational diagram of the predistorter is shown in Fig. 2. For the two-tone input, the balanced I/Q signals are given by

$$S_I = S_{IN} = A_1 \cdot \cos(\omega_1 t) + A_2 \cdot \cos(\omega_2 t) \quad (1)$$

$$S_Q = A_1 \cdot \cos\left(\omega_1 t + \frac{\pi}{2}\right) + A_2 \cdot \cos\left(\omega_2 t + \frac{\pi}{2}\right). \quad (2)$$

$H_I$  and  $H_Q$  signals consist of the second- and fourth-order terms

$$\begin{aligned} H_I &= H_2 \cdot A_{2I} + H_4 \cdot A_{4I} \\ &= A_2 A_1 G_d A_{2I} \cos[(\omega_2 - \omega_1)t] \\ &\quad + \frac{1}{2} A_2^2 A_1^2 G_d^2 A_{4I} \cos[(2\omega_2 - 2\omega_1)t] \end{aligned} \quad (3)$$

$$\begin{aligned} H_Q &= H_2 \cdot A_{2Q} + H_4 \cdot A_{4Q} \\ &= A_2 A_1 G_d A_{2Q} \cos[(\omega_2 - \omega_1)t] \\ &\quad + \frac{1}{2} A_2^2 A_1^2 G_d^2 A_{4Q} \cos[(2\omega_2 - 2\omega_1)t] \end{aligned} \quad (4)$$

where  $A_{2I}$  and  $A_{2Q}$  are the gains of the voltage-controlled VGAs for the second-order components, which could exhibit positive as well as negative polarity.  $A_{4I}$  and  $A_{4Q}$  are the fourth-order component amplification factors including multiplier.  $G_d$  is the second-order nonlinear transfer function coefficient of the detector.

The in-phase and quadrature parts of the IM generator functions are as follows:

$$\overline{S_I} = S_I + G_m \cdot S_I \cdot H_I \quad (5)$$

$$\overline{S_Q} = S_Q + G_m \cdot S_Q \cdot H_Q \quad (6)$$

where  $G_m$  is the second-order cross-modulation coefficient of the IM generator. The final output is an in-phase combination of in-phase and quadrature modulated signals. For simplicity, the final output  $S_{OUT}$  can be represented as a phasor form with a frequency component as an index as follows:

$$\begin{aligned} S_{OUT, \omega_1} &= \overline{S_{I, \omega_1}} + \overline{S_{Q, \omega_1}} \\ &= A_1 \angle 0^\circ + A_1 \angle 90^\circ \end{aligned} \quad (7)$$

$$\begin{aligned} S_{OUT, \omega_2} &= \overline{S_{I, \omega_2}} + \overline{S_{Q, \omega_2}} \\ &= A_2 \angle 0^\circ + A_2 \angle 90^\circ \end{aligned} \quad (8)$$

$$S_{OUT, 2\omega_2 - \omega_1} = G_m G_d A_1 A_2^2 [A_{2I} \angle 0^\circ + A_{2Q} \angle 90^\circ] \quad (9)$$

$$S_{OUT, 2\omega_1 - \omega_2} = G_m G_d A_1^2 A_2 [A_{2I} \angle 0^\circ + A_{2Q} \angle 90^\circ] \quad (10)$$

$$S_{OUT, 3\omega_2 - 2\omega_1} = \frac{1}{2} G_m G_d^2 A_1^2 A_2^3 [A_{4I} \angle 0^\circ + A_{4Q} \angle 90^\circ] \quad (11)$$

$$S_{OUT, 3\omega_1 - 2\omega_2} = \frac{1}{2} G_m G_d^2 A_1^3 A_2^2 [A_{4I} \angle 0^\circ + A_{4Q} \angle 90^\circ] \quad (12)$$

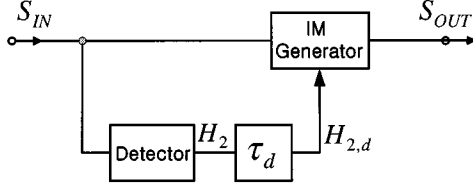
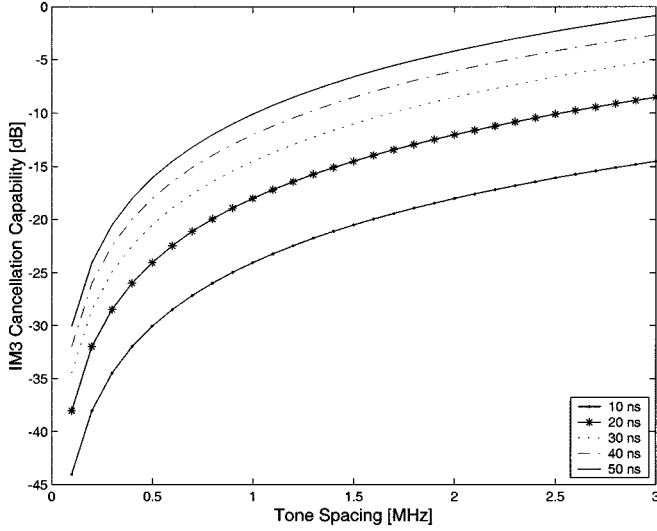
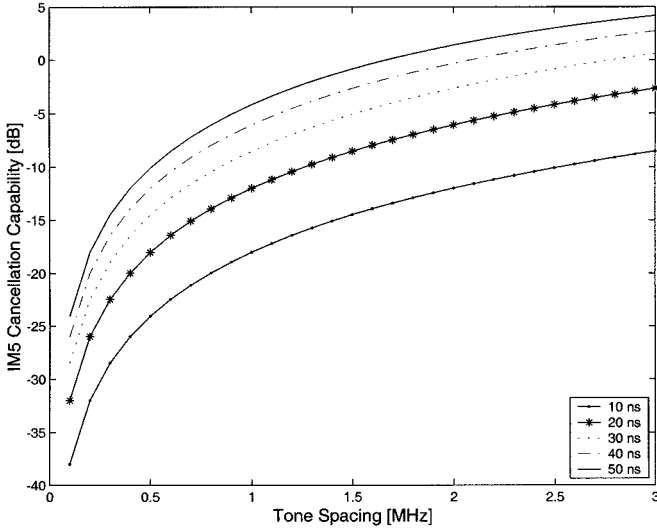


Fig. 4. Simplified block diagram to analyze the delay mismatch effect.



(a)



(b)

Fig. 5. Calculated cancellation capability versus the fundamental tone spacing for the various mismatched delays. (a) For the IM3 cancellation capability. (b) For the IM5 cancellation capability.

Since the magnitudes and polarities of  $A_{2I}$ ,  $A_{2Q}$ ,  $A_{4I}$ , and  $A_{4Q}$  can be adjusted, there is freedom to independently control the magnitudes and phases of the IM3 ( $\mathbf{S}_{OUT, 2\omega_2 - \omega_1}$ ,  $\mathbf{S}_{OUT, 2\omega_1 - \omega_2}$ ) and IM5 ( $\mathbf{S}_{OUT, 3\omega_2 - 2\omega_1}$ ,  $\mathbf{S}_{OUT, 3\omega_1 - 2\omega_2}$ ), respectively. However, the fundamental components of  $\mathbf{S}_{OUT, \omega_1}$  and  $\mathbf{S}_{OUT, \omega_2}$  do not fluctuate due to the different magnitude and phase adjustment of the IM3 and IM5 terms since  $A_1$ ,  $A_2$ ,  $G_m$ , and  $G_d$  are constants.

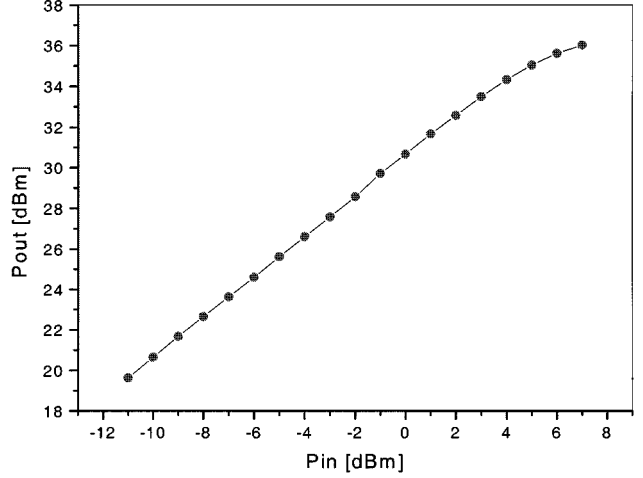


Fig. 6. Main amplifier characteristics when a single tone is applied.

### B. Predistorter Using a Double-Balanced Diode Mixer

Fig. 3 shows the block diagram of the predistorter using a double-balanced mixer as an IM generator. The detection circuit and multiplier to generate the low-frequency fourth-order term are the same as the first type. However, the IM3 and IM5 generation and control paths are different. The amplitudes of IM3 and IM5 are adjusted at the low frequency using a VGA and the phases are adjusted at the RF band.

The input signal is split into the fundamental and the error generation paths. The signal in the error generation path is split again into the IM3 and IM5 generation paths. In the IM3 generation path, the signal is injected to the local-oscillator (LO) port of the double-balanced diode mixer, then is mixed with the IF port signal, which is the detected and amplified low-frequency  $\omega_2 - \omega_1$  component. A pure IM3 signal is generated at the RF port due to the port isolation characteristics of the double-balanced mixer. Therefore, any complex cancellation circuits for the fundamental signal in the IM generation paths are not required in this case.

As in the same way as the IM3, the IM5 is generated from the  $2\omega_2 - 2\omega_1$  component. These IM signals are combined with the main signal after independent phase adjustment. This predistorter has simpler low-frequency circuits and a little more complex RF circuits than the first type using an I/Q balanced modulator.

## III. DELAY MISMATCH EFFECT

To analyze the delay mismatch effect of the predistortion circuits described in the previous section, a simplified block model is used, as shown in Fig. 4. For simplicity, the second-order coefficients of the transfer functions of the detector and IM generator are assumed to be unity. Let the mismatched delay of the low-frequency circuit be  $\tau_d$ . The delayed low-frequency second-order term is given as

$$H_{2,d} = \cos [(\omega_2 - \omega_1)t - (\omega_2 - \omega_1)\tau_d]. \quad (13)$$

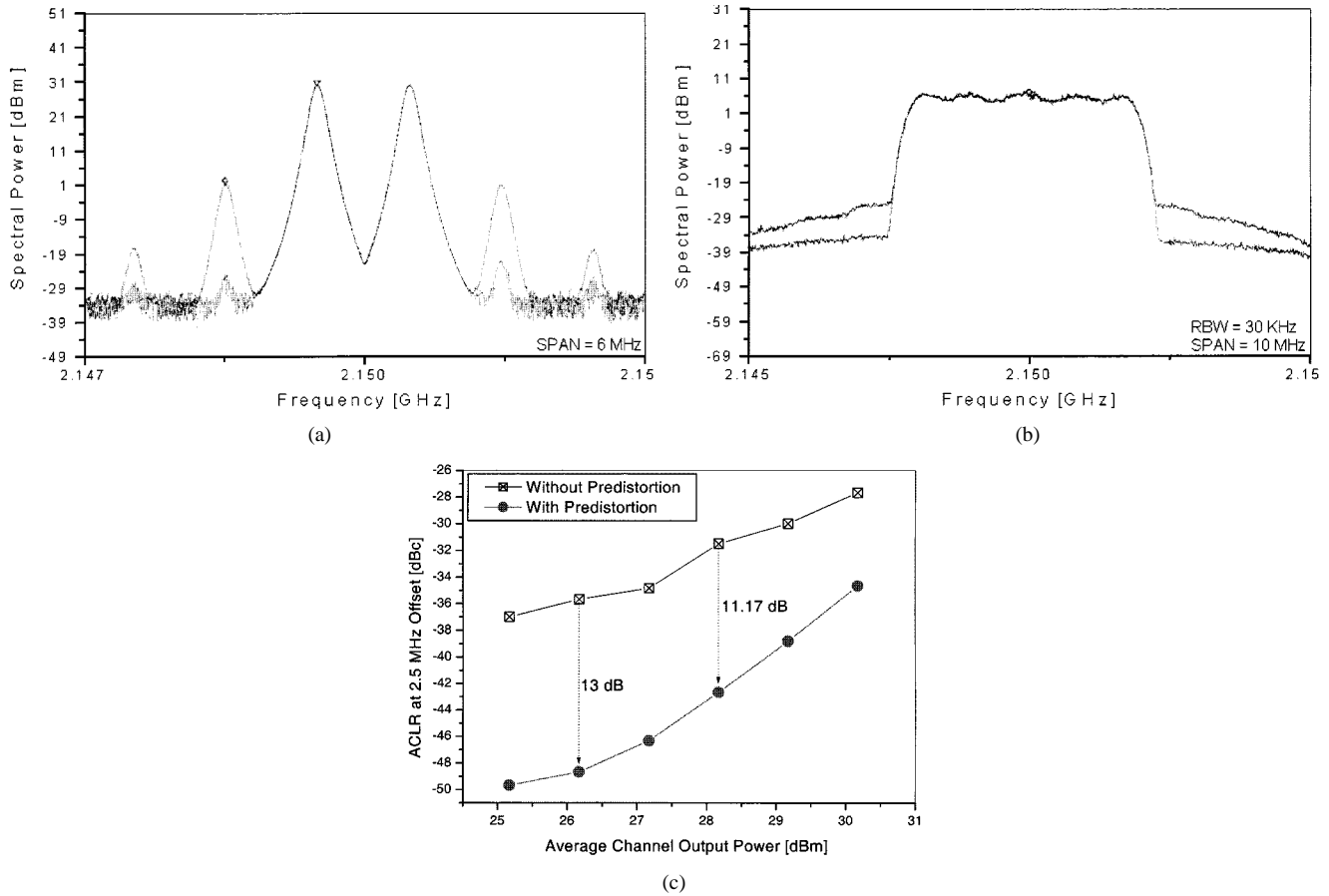


Fig. 7. Linearization results of the predistorter using an I/Q balanced modulator. (a) For a two-tone test spectra. (b) For a broad-band CDMA spectra with a chip rate of 4.096 Mc/s and an average output channel power of 28.17 dBm. (c) For ACLR versus average output channel power of a broad-band CDMA signal at 2.5-MHz offset frequency.

The  $S_{\text{OUT}}$ 's of the IM3 components are represented as

$$S_{\text{OUT}, 2\omega_2 - \omega_1} = 1 \angle -(\omega_2 - \omega_1)\tau_d \quad (14)$$

$$S_{\text{OUT}, 2\omega_1 - \omega_2} = 1 \angle (\omega_2 - \omega_1)\tau_d. \quad (15)$$

From (14) and (15), the phase of the upper part ( $S_{\text{OUT}, 2\omega_2 - \omega_1}$ ) of the IM3 is decreased by  $(\omega_2 - \omega_1)\tau_d$  and the phase of the lower part ( $S_{\text{OUT}, 2\omega_1 - \omega_2}$ ) increases by the same amount. This property could lead to a serious performance degradation: limitation on the amount of cancellation and cancellation unbalance between the upper and lower part of the IM3.

In the same way of the IM3, the effect of the phase mismatch of IM5 due to the delay  $\tau_d$  can be calculated as

$$S_{\text{OUT}, 3\omega_2 - 2\omega_1} = 1 \angle -2(\omega_2 - \omega_1)\tau_d \quad (16)$$

$$S_{\text{OUT}, 3\omega_1 - 2\omega_2} = 1 \angle 2(\omega_2 - \omega_1)\tau_d. \quad (17)$$

Equations (16) and (17) show that the IM5 cancellation is twice as sensitive to the phase mismatch than the IM3 cancellation. This delayed mismatch effect is somewhat different from that of the well-known feedforward system.

Fig. 5 is the calculated cancellation capability versus the fundamental tone spacing for the several mismatched delays: Fig. 5(a) for the IM3 and Fig. 5(b) for the IM5. As shown, the IM3 and the IM5 cancellation capabilities are seriously restricted and the performance is more seriously degraded as

the delay mismatch increases and the tone spacing becomes wider.

#### IV. EXPERIMENTAL RESULTS

To validate the proposed predistortion linearizers, two types of the predistorters are implemented. In both cases, we have used the same detection circuits. They consist of Mini-circuit's ERA-5SM as a low-frequency second-order IM generator, a 50- $\Omega$  load resistor as an RF termination, an RF choke inductor, a series inductor, a resistor to choke a detected  $\omega_2 - \omega_1$  signal, and a large capacitor to bypass the detected signal. The analog circuits including a multiplier, voltage-controlled VGA, and adder are designed to have at least 25-MHz bandwidth for broad-band linearization. The VGA was designed to have a positive or a negative gain polarity according to the control voltage. The analog circuits' delay is compensated by a coaxial delay line, which is about 18 ns in this experiment.

The IM generation circuit of the first type consists of varactor diodes connected to a reflection-type 90° hybrid coupler. The dc bias is properly assigned to the varactor diodes to prevent generation of any higher order components since only the second-order coefficient of the phase modulation characteristics of the varactor diode is used.

In the predistortion linearizer using a double-balanced diode mixer, an RF phase shifter is built using varactor diodes in re-

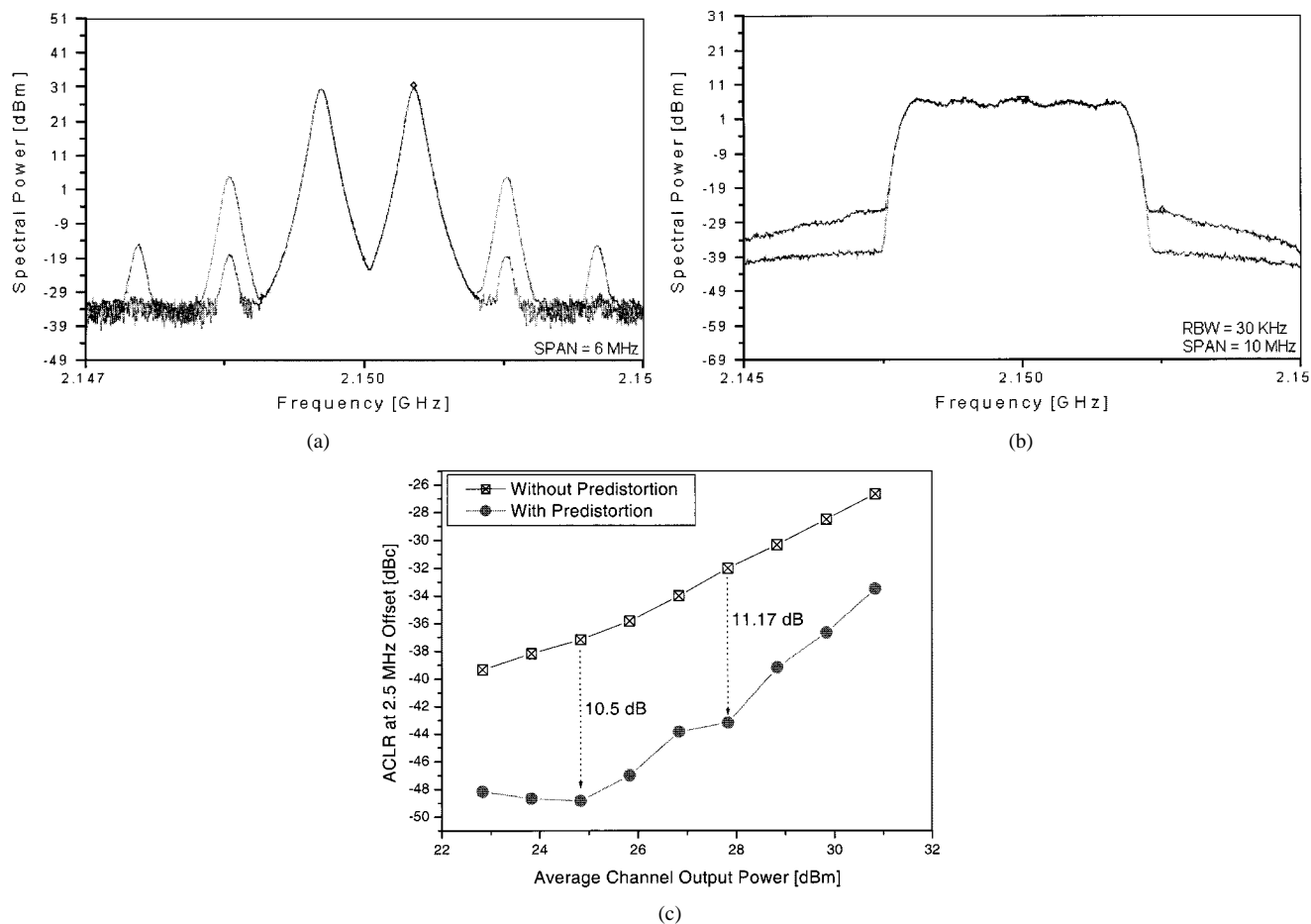


Fig. 8. Linearization results of the predistorter using a double-balanced mixer. (a) For a two-tone test spectra. (b) For a broad-band CDMA spectra with a chip rate of 4.096 Mc/s and an average output channel power of 28.83 dBm. (c) For ACLR versus average output channel power of a broad-band CDMA signal at 2.5-MHz offset frequency.

flection type to have more than a 180° tuning dynamic range. The double-balanced mixer is RF prime’s RFMT-25H. Delay line 1 compensates for the low-frequency circuit delay and delay line 2 compensates for the delay of the mixer and phase shifter.

In this experiment, the main amplifier is composed of a single driver stage and a final power stage (Motorola’s MHL21336, 35-dBm amplifier) with a total gain of 30.7 dB. Fig. 6 shows the in-out characteristics of the main amplifier when a single tone is applied. This main amplifier is linearized using the two proposed predistorters.

Fig. 7 shows the linearization results of the first type of predistorter. When a two-tone signal with 1-MHz spacing is applied to the amplifier with 33.17-dBm output power, the IMD3 is improved by over 23 dB and the IMD5 is improved by approximately 10 dB to near spurious level [see Fig. 7(a)]. Linearization with a two-tone signal provides the initial control voltages of the VGAs to optimize the performance for a CDMA signal. When a broad-band CDMA signal with a chip rate of 4.096 Mc/s and a crest factor of 11 dB is applied to this test circuit, the adjacent channel leakage power (ACLR) is improved by over 11.17 dB. In this case, the average output power is 28.17 dBm at a center frequency of 2.15 GHz [see Fig. 7(b)]. When the average power level of the CDMA signal is swept, the ACLR improvement variations are plotted in Fig. 7(c). It shows good cancellation properties for a broad range of output power.

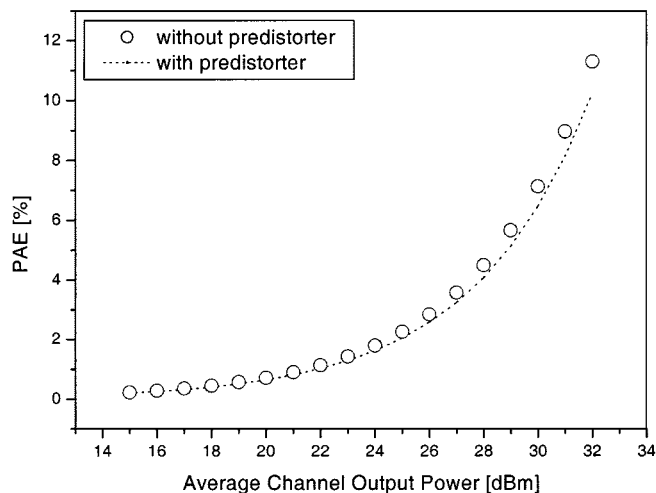


Fig. 9. Measured PAE of the amplifier without the predistorter (circles) and with the predistorter (dotted line).

Similar tests were performed for the second type of linearizer. Fig. 8 shows the results. For the same two-tone test, IMD3 is improved by over 23 dB and the IMD5 is improved by over 17 dB near to the spurious level [see Fig. 8(a)]. As shown in Fig. 8(b), the ACLR test delivers about 11.17-dB improvement. The performances of the two predistorters are quite similar.

A very low power consumption of the predistorter by dealing with a very low RF power in the input stage makes little degradation of the overall efficiency from that of the power amplifier itself. Hence, the efficiency of the amplifier using predistortion is clearly better than that of the feed-forward amplifier. Fig. 9 shows the power-added efficiency (PAE) versus average channel output power of the amplifier by applying CDMA signal. The PAE is slightly degraded by the static power consumption of the predistorter by including low-frequency circuits, which is fixed to 1.44 W, in comparison to without the predistorter case. As the output power capacity of the amplifier for linearization increases, the efficiency degradation due to a static power consumption caused by the predistorter becomes negligible.

## V. CONCLUSIONS

We have discussed the three performance degradation factors of predistortion in comparison with the feed-forward method. These factors offer an explanation of the cancellation limit of the predistorter and provide a design guide for a linear power-amplifier adopting predistortion linearizer. New predistortion techniques using a low-frequency even-order IM components have been proposed. Two types of linearizers, one using an I/Q balanced modulator and the other using a double-balanced diode mixer, have been implemented. These linearizers have a very compact circuit configuration and low gain losses. Both circuits are able to independently control the magnitudes and phases of the IM3 and IM5 components.

We have analyzed the delay mismatch effect of the predistorter. The results show that the IM5 is twice as sensitive than the IM3 for the delay mismatch. This result is applicable to other predistortion circuits as well.

To validate the proposed predistortion linearizers, a two-tone linearization test and a broad-band CDMA linearization test are performed at the IMT-2000 band of 2.15 GHz. The results show that significant cancellations are achieved for both the IM3 and IM5 components. The broad-band CDMA test and its power sweeping test show that the ACLR is improved by over 11.17 dB at an optimized average channel output power and the improvement is maintained through a broad range of the power levels. These predistorters can be easily linked into appropriate adaptation control circuits because both circuits use only four control parameters and the compact sizes of the predistorters are convenient for adding spaces for adaptive control circuits.

## REFERENCES

- [1] Y. Yang, Y. Kim, J. Yi, J. Nam, B. Kim, W. Kang, and S. Kim, "Digital controlled adaptive feedforward amplifier for IMT-2000 band," in *IEEE MTT-S Int. Microwave Symp. Dig.*, vol. 3, Boston, MA, June 2000, pp. 1487–1490.
- [2] J. K. Cavers, "Adaptation behavior of a feedforward amplifier linearizer," *IEEE Trans. Veh. Technol.*, vol. 44, pp. 31–40, Feb. 1996.
- [3] E. E. Eid and F. M. Ghannouchi, "Adaptive nulling loop control for 1.7 GHz feedforward linearization systems," *IEEE Trans. Microwave Theory Tech.*, vol. 45, pp. 83–86, Jan. 1997.
- [4] K. Konstantinou and D. K. Paul, "Analysis and design of broadband, high efficiency feedforward amplifiers," in *IEEE MTT-S Int. Microwave Symp. Dig.*, May 1996, pp. 867–870.
- [5] S. Kumar and G. Wells, "Memory controlled feedforward lineariser suitable for MMIC implementation," *Proc. Inst. Elect. Eng.*, pt. H, vol. 138, no. 1, pp. 9–12, Feb. 1991.

- [6] R. G. Meyer, R. Eschenbach, and W. M. Edgerley, "A wide-band feed-forward amplifier," *IEEE J. Solid-State Circuits*, vol. 9, pp. 422–428, Dec. 1974.
- [7] A. Katz, "SSPA linearization," *Microwave J.*, vol. 42, no. 4, pp. 22–44, 1999.
- [8] Y. Kim, Y. Yang, S. Kang, and B. Kim, "Linearization of 1.85 GHz amplifier using feedback predistortion loop," in *IEEE MTT-S Int. Microwave Symp. Dig.*, 1998, pp. 1675–1678.
- [9] J. Yi, Y. Yang, M. Park, W. Kang, and B. Kim, "Analog predistortion linearizer for high power RF amplifier," in *IEEE MTT-S Int. Microwave Symp. Dig.*, vol. 3, Boston, MA, June 2000, pp. 1511–1514.
- [10] S. P. Stapleton and F. C. Costescu, "An adaptive predistorter for a power amplifier based on adjacent channel emission," *IEEE Trans. Veh. Technol.*, vol. 41, pp. 49–56, Feb. 1992.
- [11] K. Yamauchi, K. Mori, M. Nakayama, Y. Itoh, Y. Mitsui, and O. Ishida, "A novel diode linearizer for mobile radio power amplifiers," in *IEEE MTT-S Int. Microwave Symp. Dig.*, 1996, pp. 831–834.
- [12] P. B. Kenington, S. J. Gillard, and A. E. New, "An ultra-broadband power amplifier using dynamically controlled linearization," in *IEEE MTT-S Int. Microwave Symp. Dig.*, 1999, pp. 355–358.
- [13] E. G. Jeckeln, F. Beaugerard, M. A. Sawan, and F. M. Ghannouchi, "Adaptive baseband/RF predistorter for power amplifiers through instantaneous AM-AM and AM-PM characterization using digital receivers," in *IEEE MTT-S Int. Microwave Symp. Dig.*, 2000, pp. 489–492.
- [14] C. G. Rey, "Adaptive polar work-function predistortion," *IEEE Trans. Microwave Theory Tech.*, vol. 47, pp. 722–726, June 1999.
- [15] H. Kawasaki, T. Ohgihara, and Y. Murakami, "An investigation of IM3 distortion in relation to bypass capacitor of GaAs MMIC's," in *IEEE Microwave Millimeter-Wave Monolithic Circuit Symp. Dig.*, 1996, pp. 119–122.
- [16] W. Bosch and G. Gatti, "Measurement and simulation of memory effects in predistortion linearizers," *IEEE Trans. Microwave Theory Tech.*, vol. 37, pp. 1885–1890, Dec. 1989.



**Youngoo Yang** (S'99) was born in Hamyang, Korea, in 1969. He received the B.S. degree in electronic engineering from Han-Yang University, Ansan, Korea, in 1987, and is currently working toward Ph.D. degree at the Pohang University of Science and Technology (POSTECH), Namku Pohang, Korea.

His research interests include linearization techniques and behavioral modeling of high-power amplifiers, large-signal modeling of microwave devices, and RF integrated circuit (RFIC) design.



**Young Yun Woo** was born in Taegu, Korea, in 1976. He received the B.S. degree in electronic and electrical engineering from Han-Yang University, Seoul, Korea, and is currently working toward the M.S. degree at the Pohang University of Science and Technology (POSTECH), Namku Pohang, Korea.

His current research interests include RF power amplifier design and low-power amplifier (LPA) control circuits design.

**Bumman Kim** (S'77–M'78–SM'97) received the Ph.D. degree in electrical engineering from the Carnegie–Mellon University, Pittsburgh, PA, in 1979.

From 1978 to 1981, he was involved with fiber-optic component research at GTE Laboratories Inc. In 1981, he joined the Central Research Laboratories, Texas Instruments Incorporated, where he was involved in development of GaAs power FETs and monolithic microwave integrated circuits (MMICs). He developed a large-signal model of a power FET, dual-gate FETs for gain control, and high-power distributed amplifiers, and various millimeter-wave MMICs. In 1989, he joined the Pohang University of Science and Technology (POSTECH), Namku Pohang, Korea, where he is currently a Professor in the Electronic and Electrical Engineering Department and Director of the Microwave Application Research Center, where he is involved with device and circuit technology for MMICs. He has authored or co-authored over 100 technical papers in this area.

Dr. Kim is a member of the Korean Academy of Science and Technology.